A numerical study of the pressure applied on CFRP panels during a lightning strike using a coupled electro-thermal-mechanical model

Christine Espinosa, T. Montel, J.F. Montes Pons, Frederic Lachaud, F. Soulas

A numerical study of the pressure applied on CFRP panels during a lightning strike using a coupled electro-thermal-mechanical model

Christine Espinosa*, Thomas Montel, José Montes Pons, Fréderic Lachaud, Floriane Soulas

** Institut Clément Ader (ICA), Université de Toulouse, CNRS-INSA-ISAE-Mines Albi-UPS,*
3 Rue Caroline Aigle, 31077 Toulouse Cedex 4, France
Christine.espinosa@isae-supaero.fr

Keywords: lightning, damage, electro-thermo-dynamic coupling, composite material, numerical model.

Abstract

The damage generated as direct effect of a lightning strike on a composite panel is of primary interest in aeronautics. Interactions between the protection layers and the composite during lightning are not well known. This work aims at evaluating the pressure and temperature that is applied onto the composite panel by the protection layers during the lightning. A 3D fully coupled electromagnetic-thermal-mechanical numerical model is proposed. A D-wave current is injected in time on the metallic mesh external surface. The current injection surface evolves in time following a prescribed burning process. Resulting Joule effects generated in the metallic mesh are responsible of high pressures and temperatures transmitted to the underlying composite panel. The resulting computed pressure and temperatures are outputs of the simulation. Amplitudes in space and time of the resulting pressure on the surface of the composite panel are compared to models found in the literature.

1 Introduction

To reduce the direct mechanical damage caused by lightning on the composite structures of new generation aircraft, these structures are protected by metal coatings. We are interested here in metal structures of type grid of copper in a resin layer. Loadings under interest are D-current wave forms. Optimizing the design of protection structures requires a thorough understanding of individual and action combined parameters that drive their performance to evacuate the current, and to reduce structural damage in composite panels. However it is very difficult experimentally to establish this relationship. One of the reasons is that the damage in composite plates is a nonlinear phenomenon that interacts with the progressive destruction of the metallic mesh. If the certification gives instructions for the issued current (ED84, ED105), the process of the metal shield destruction is not measurable, even the chronology of creation and propagation of the damage in composite plate as and to the extent of the destruction of the metallic mesh.

There are more and more work in the literature seeking to determine damages in composite structures to lightning shocks. Very little focus on structures coated and painted. Our focus is on the founding experimental work which sought to establish thermodynamic models based on energy equivalence to define the aggression suffered by the composite panels [1-5]. A model proposed by [6,7], similar to the work of [8,9] indicates that this impulse can be modelled by equivalent pressure. This pressure profile is similar to that of an explosion, reminiscent of the recent work of Liu [10] and [11] Dong. In the works of Liu including two simulations are carried out. The first makes an electro-thermal coupling to calculate the heating by Joule effect produced by the flow of the current. The second uses the heat in a thermodynamic calculation to calculate the pressure of explosion induced by using an equation of State of JWL. The surface of injection does not evolve in these two studies, unlike the experimental observations conducted recently by ONERA [12].
The purpose of this work is to propose a model of strongly coupled simulation electro magneto-thermo-dynamics of current injection by varying the surface of injection in order to model the progressive evaporation of the grating of copper due to the Joule effect. The model is based on an energy equivalency to calculate changes in the radius of injection. It uses the implicit electromagnetic solvers, thermal dynamic and implicit explicit code of LS - Dyna® in a manner strongly coupled. Produced by the injection pressure and temperature are calculated in a single numerical calculation. The pressure and temperature obtained are compared with the results of the literature. If improvements are needed on the representation of the behaviour of materials, notably to take into account the variation of properties depending on the temperature, we demonstrate that the methodology is robust and offers interesting opportunities to understand the contribution each and simultaneous electric, thermal and hydrodynamic components of composite plate.

2 Experimental case of reference

Experimental cases of reference are presented in [13,8]. Composite plates have lateral dimensions of 450 mm x 450 mm, and are fixed by 12 equidistant bolts placed on a circle of diameter 370 mm. The plates are quasi-isotropic composite laminates made of eight T800/M21 plies with stratification [45/0/-45/90]s. The final thickness is 2mm. They are coated

with a layer of Expanded Copper Foil embedded in an epoxy resin of surface mass 195 g/m² (ECF1953Cu7 - 100a DEXMET) and of 127µm in thickness. The ECF-resin coating is covered with a layer of paint of 200µm thickness. The plates have undergone a D-shape current waveform of intensity 95-100kA in 20µs, with a total duration of about 100µs.

3 Scalable current injection surface

In order to model the load that applies both on a wire fence on a continuous sheet, the model proposed here is to inject intensity over time on an annular surface. The ring area is bounded by two rays that evolve in time. These two rays delineate the area through which current can be injected into the metal protection as it is sprayed (Figure 1).

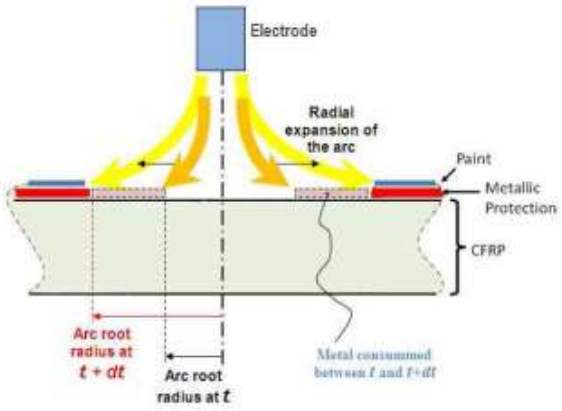

Figure 1 Radial expansion of the arc-root column [6]

This hypothesis assumes that the current passes from privileged in metal protection rather than in the first composite fold way. This assumption is no longer valid if the first trick composite resin has been melted and let carbon fibre Strip. In this case current could pass also in carbon fibres and cause an explosion of surface charge of important decking in the first interfaces, similar to what is caused by a current more low intensity on a naked CFRP [2, 10]. This last scenario is not taken into account in the present study. Only the Joule effects are considered here. The injection is the consumed metal area described by Lepetit [6].

The qualitative arc root growing scenario identified from previous works of Lepetit [6] and Karch [9] is implemented into a quantitative arc root model providing time dependent damaged surface area and possibly a post-strike damage area prediction. For the sake of exploratory modelling, a first set of hypothesis was assumed: Joule effect was the only source of energy deposited into the metallic protection and heat transfer as well as acoustic pressure effects from the arc were neglected, which is typically one order of magnitude smaller. A metal protection, with thickness e [m], surface density δ [kg/m²], volume density ρ [kg/m^3], and electrical conductivity σ (S.m^{-1}) is considered. The objective is to reproduce the expansion of the arc root r(t) expressed as a growing damage area of the metallic mesh. This vanishing crown is considered completely sublimated at a time t(r) when it would have absorbed a quantity of energy given by ρ ΔH 2πerdr, where ΔH is the enthalpy of fusion (or vaporization) [J/kg]. The smallest radius is given by the melted or vaporized area. The larger radius corresponds to the area which begins to heat up by Joule effect beyond the ambient temperature. The highest temperature giving the internal radius is chosen to be equal to 1000 ° C, which is approximately the temperature of fusion of copper. The evolution of molten rays with time is given by equation (1). The two rays are calculated for each of the copper resistivity at 20 ° C (1/σ(T)=1.68 10^{-8} Ωm) and at 1000°C (1/σ(T)=13.1 10^{-8} Ωm).

$$r(t) = \frac{1}{2\pi\delta}\left(\frac{1.7\rho\int_0^t \frac{1}{\sigma(T)} I(\tau)^2 d\tau}{\Delta H}\right)^{\frac{1}{2}} \quad (1)$$

Where I(t) is the D-wave delivered current in time that reaches 100kA at 20µs and lasts about 100µs:

$$I(t) = 6.58\,10^6\,(e^{-50000t} - e^{-52000t}) \quad (2)$$

3 Numerical model

We use the three strongly coupled solvers of the LS-DYNA® code [14,15]. The electromagnetic Solver solves the equations of Maxwell with an implicit method. This Solver uses a calculation by finite elements (FEM) to calculate the spread of currents inside the drivers volumes, and a method of boundary elements (BEM) to calculate the effect induced in conductors items that receive the electromagnetic loading (via the faces). The use of the BEM avoids calculating the spread of currents in the air, so do not do a calculation of fluid mechanics to determine the spread of the loading. The thermal Solver solves the equations of heat, namely the conservation of energy and the heat conduction equation. The thermal Solver is implied. The mechanical Solver solves the equation of propagation of waves in explicit dynamics. To pair the three solvers of terms are added in the equations, a term of the Lorentz force in mechanical, and a term of energy due to the Joule effect in thermal energy conservation equation [14].

3.1 Geometry and mesh

The sample is chosen smaller than the real plate for computation time reasons. The thermal and the electromagnetic (EM) solvers use implicit time integration schemes, and the Boundary Element matrix used by the EM solver is computed as and extent of deformation. Dimensions of the sample plate were chosen in order to reduce the CPU time without disrupting the calculations during loading.

The model presented here is a square plate of 108 mm x 108 mm lateral dimensions smaller than the actual plates (Figure 2). Each composite ply is meshed with eight nodes solid elements with three degrees of freedom per node, and a reduced integration in thickness.

The small size of the grating geometry is not represented with real shape and size. A rectangular model is created to simplify the calculations. This model is composed of spaced copper

bars forming a rectangular grid (in blue on Figure 3) filled with resin (green on Figure 3).

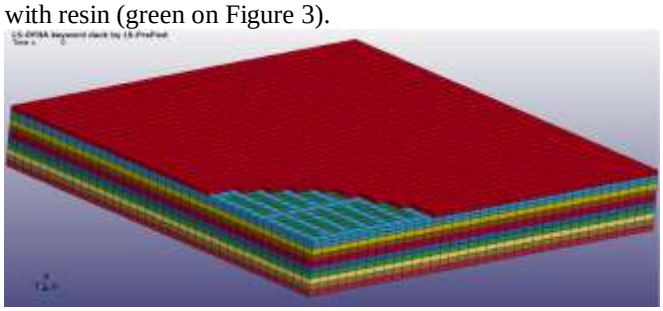

Figure 2 : ¼ of the composite plate finite element model

The number of bars in x direction (//0° composite plies) and y direction (//90° plies) is calculated to meet the surfaces covered by copper and resin and the prescribed ratio of electrical resistance given by DEXMET (Figure 3, [16]). The width of each bar is adjusted to a=b=l=0.5 mm which is the size of the mesh of the composite plate to ensure a perfect continuity using common nodes. In order to get the x and y resistivity equivalent to that of the real ECF geometry, the conductivity is set isotropic in the finite elements copper bars and the number of bars in the x and y directions is calculated so as to ensure the electrical conductivity meet the real ECF one. In this way a unique conductivity σ is introduced into the software and the anisotropy of conductivity is provided by the grid geometry. The methodology is detailed by equations (3) to (7). The total resistance in x (/ y) direction is given by equation (3), where Rxi (/ Ryi) represents the electrical resistance of one bar in x (/ y) direction given by equation (4), and σ the electrical conductivity.

$$\frac{1}{R_x} = \sum_i \frac{1}{R_{x_i}} \qquad (3)$$

$$R_{x_i} = \frac{L_x}{\sigma \cdot S_x} = \frac{L_x}{\sigma \cdot b \cdot e} \qquad (4)$$

This allows writing for a square plate (Lx=Ly=L):

$$\frac{1}{R_x} = \sum_i \frac{\sigma \cdot b_i \cdot e}{L_x} = \frac{\sigma \cdot e}{L_x} \cdot n_x \cdot b = \frac{\sigma \cdot e}{L} \cdot n_x \cdot l \quad (5)$$

$$\frac{1}{R_y} = \sum_i \frac{\sigma \cdot a_i \cdot e}{L_y} = \frac{\sigma \cdot e}{L_y} \cdot n_y \cdot a = \frac{\sigma \cdot e}{L} \cdot n_y \cdot l \quad (6)$$

The real ECF being anisotropic in shape, the ratio of resistance in x and y is about 3 [16], the ratio of number of bars of same width l in x and y directions is set to 3, leading to the geometry illustrated on Figure 3:

$$\frac{R_x}{R_y} = \frac{n_y}{n_x} = f \approx 3 \qquad (7)$$

The ECF layer contains two elements in the thickness in order to let the current flow in the thickness and exit at the boundaries. To keep a reasonable calculation times, the thickness of the layer of ECE has been slightly enlarged to e=0.037mm. The edge of the plate is surrounded by a continuous copper bar in order to ensure the continuity of the current.

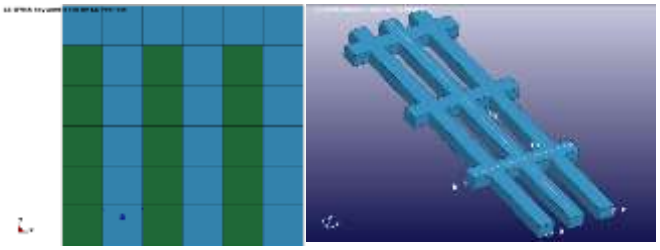

Figure 3 : Elementary shape of the metallic mesh model

Finally the paint layer is meshed with the same finite elements square mesh in the plate plan, and one solid element in the thickness of 200µm. To both represent the disappearance of the painting that can be observed after real tests, and apply the loading in the form of issued on the upper surface intensity, an unpainted area is modelled in the form of a disc of 6 mm of total radius.
The model includes 620 000 nodes, 350000 solid elements.

2.2 Material behaviour

The behaviour of the four different materials must be defined for each solver: electromagnetic, thermal and mechanical.
The composite plies are supposed to be electrically conductive with an isotropic conductivity σ=0.01 $\Omega^{-1}.mm^{-1}$. Their mechanical behaviour and thermal behaviour are both orthotropic elastic. The thermal properties are set linearly dependent on the temperature. Data for both anisotropic behaviour laws are given in **Erreur ! Source du renvoi introuvable.**.

Elastic ply properties	
E_{11}	112 GPa
E_{22}	7.64 GPa
E_{33}	7.64 GPa
ρ	1550 kg/m^3
$\nu_{12}\nu_{13}$	0.35
ν_{23}	0.4
G_{12}	5.61 GPa
G_{13}	5.61 GPa
G_{23}	2.75 GPa

Thermal orthotropic	
h_c	1110
k_1	6.09 10^{-4}
k_2	6.09 10^{-4}
k_3	0.0118
Tmu	6 10^{-6}

Table 1 : Composite material parameters

The copper grid is electrically conductive. For a thickness of e=0.037 mm, the equivalent electrical conductivity is worth about σ=9008$\Omega^{-1}.mm^{-1}$. The density is adjusted to 0.0089 g/mm² to meet the surface weight of the real ECF195.
The Johnson Cook material model and Mie-Grüneisen equation of state are used for the copper mechanical behaviour. The data are listed in the following tables.

ρ	E	ν	Tm	P_c	$\dot{\bar{\varepsilon}}_0$
8.9	110	0.33	1083	-13	1
g cm^{-3}	GPa		°C	MPa	

Table 2 Johnson-Cook damage parameters for the copper

A	B	C	n	m	$\dot{\bar{\varepsilon}}_0$
90	292	0.025	0.31	1.09	1
MPa	MPa				

Table 3 Johnson-Cook flow stress parameters for the copper

α(Thermal expansion)	*Specific heat*	*Thermal conductivity*
17 μK^{-1}	500J/(Kg*K)	390 W/(m*K)

Table 4 Thermal parameters for the copper

The epoxy resin contained within the copper bars grid, and the paint that covers all, have both a linear elastic mechanical behaviour and insulating thermal behaviour. They are electrically insulating. The resin has a density of 1285kg/m3, a Young modulus of 3 MPa, and a Poisson ratio of 0.3. The specific heat is 1300 J/(Kg*K), and thermal conductivity is 1.2 W/(m*K). The paint has a density adjusted to get the right added mass on the top, a Young modulus of 3 MPa, and a Poisson ratio of 0.3 as for the resin. The specific heat is 1758 J/(Kg*K), and thermal conductivity is 0.02 W/(m*K).

Delamination is modelled using tied interfaces between adjacent surfaces of neighbour composite plies. The links break when the yield conditions given by Equations (8) or (9) are reached.

$$\frac{\sqrt{\sigma_n^2+3|\sigma_S|^2}}{NFLS} \leq 1 \qquad \textit{in tension} \qquad (8)$$

$$\frac{\sqrt{3|\sigma_S|^2}}{NFLS} \leq 1 \qquad \textit{in compression} \qquad (9)$$

Where σ_n and σ_S respectively represent the local normal and shear stress and NFLS is the corresponding allowable yield stress. NFLS is set to 990 MPa. When the yield condition is reached, the interface undergoes a progressive cohesive damage which evolves as a function of the crack opening. The stress is scaled down by a factor which represents the damage function, starting from a value of 1 for the undamaged state and decaying to zero at the maximum width of the crack which has been set to 0.1mm.

2.3 Initial and boundary conditions

The ambient temperature is 25°C all around the sample.
The top faces of the ECF marked with a cross are the faces of the power source (current injection), and the lateral side faces of the ECF and of the composite plies are the faces of current output (Figure 4).

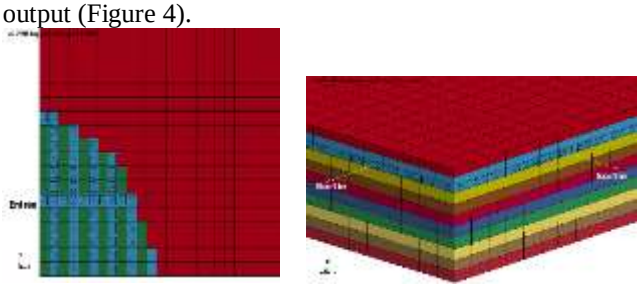

Figure 4 : Current input / output principle

2.3 Current injection model

We chose to use the resistive solver as current in the form of double exponential given by Equation 2 can be regarded as a current low frequency, and because the skin effect is negligible here. The intensity received by the ring surfaces is calculated at every moment of time from the first beginning of the current delivery up to 100µs to ensure the conservation of the total current delivered to the D Wave described by equation (2). This current is characterized by its maximum current, electric transfer workload, its rising edge and its integral of action. The proposed formula relies on the spatial discretization of the copper mesh of the numerical model. The load is imposed through time using different injection curves of varying intensity on corresponding rings of element faces. Eight set of ring shape are composed of 94 open circuits made up of adjacent sides all at the same time located between the two rays of the crown of injection (Figure 5). An example of circuits sampling in ring A is given on Figure 6.

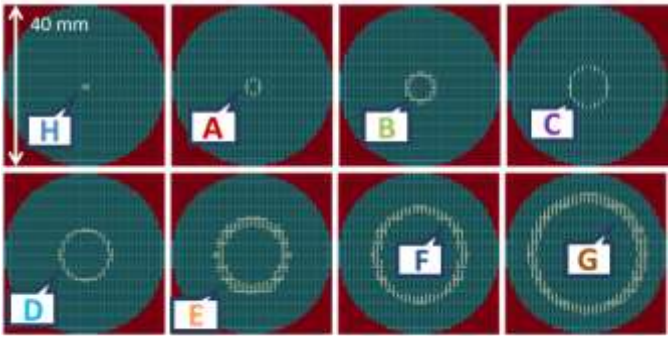

Figure 5 : Eight rings of current injection

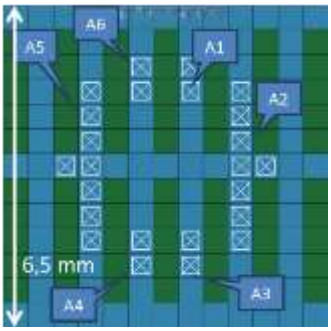

Figure 6 : Ring A composed of 6 circuits sets

Each injection circuit is defined by the minimum and maximum distance at the injection site (Table 5), and its weight is defined as the number of faces making it up.

Ring	H	A	B	C	D	E	F	G
Nb of circuits	1	6	4	18	16	8	21	19
Minimum radius (in mm)	0	1.25	2.75	4.25	5.5	7.25	10	12.75
Maximum radius (in mm)	0.5	2.25	3.75	5.25	6.75	10	12.25	15.25

Table 5 : Eight rings of current injection sets

The coarse mesh size (l=0.5mm) is the source of a coarse sampling of the current which negative effect is smoothened using a mean on 0.5µs only during the increase and decrease phases of the current. For practical reasons, a smoothing function L(t) is introduced with zero values except during these two phases. In order to equate the power received by the copper grid in the rings of injection with the power delivered by the source at each instant, and because the conductivity in

the model does not vary with the temperature in this former model, the input intensity is corrected to account for the evolution of conductivity from the room temperature to the melting temperature.

$$I_{circuit}(t) = Weight_{circuit} * \frac{L(t)}{\sum Weight_{circuit}(t)} I(t) \quad (10)$$

$$I_{modèle}(t) = I_{réel}(t)*\text{sqrt}\ (\text{délivrée} * \sigma_{20°}/\ \sigma_{1000°}) \quad (11)$$

The total delivered intensity is the sum of the eight intensity curves as described by

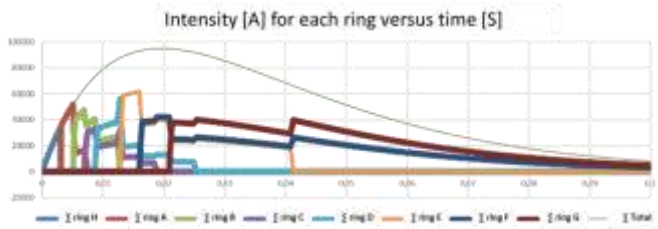

Figure 7 : Intensity over time on the eight rings

3 Results

From the beginning of the current injection into the circuits, the Joule effect produces Ohm heating in the 3D copper elements. This heat propagates to the neighboring elements by conduction, while the injected current is distributed through the common nodes in the neighboring electrically conductive elements. This phenomenon is illustrated at 10 µs after the start of injection on Figure 8. A zoom was made on the display of a quarter plate to facilitate the view of the distribution in the volume. It can be seen that the heat remains concentrated in the upper folds of the composite plate and in the copper mesh. The current is diffused isotropically (direction of the arrows). The amplitude (color and length of the arrows) is forced by the proposed injection model.

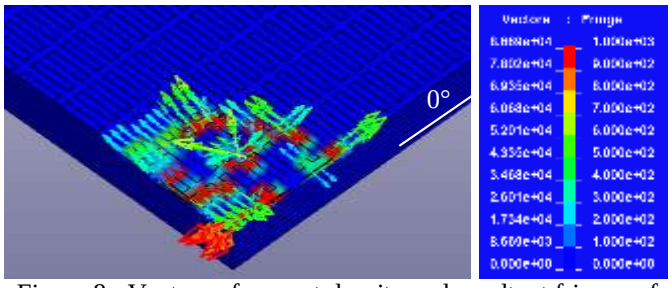

Figure 8 : Vectors of current density and resultant fringes of Ohm heating at 10µs in the coupled model

It is found that the coarse discretization of the copper mesh and the presence of electrically insulating resin cause disturbances on the direction of propagation of the current which tends to return towards the center of the plate. This return is also due to the fact that the electrical conductivity has been chosen to be constant versus temperature in this model. It is therefore not possible to model the effect of the phase change or of the vaporization of the protective layer in the center of the plate during the injection, as it is the case in the actual test. On the other hand, despite the creation of groups of faces forming isotropic concentric rings (see Figure 5), the current flow takes on an oval shape which accounts for the anisotropy of the electrical conductivity of the protective layer as the case in the actual test.

This anisotropy of the current distribution generates a slight anisotropy of the Joule heating at the periphery of the hot zone in the first composite ply directly in contact with the protective layer. It is mostly visible after the maximum current peak. In the first moments, Joule heating is quasi-isotropic. This is illustrated on Figure 9. The scale has been limited to1000°C which represents approximately the melting temperature of copper. This first ply is oriented at 45 ° and the thermal conductivities of the model being anisotropic in the composite plies, the hottest zones are also slightly disturbed by this anisotropy. This can be visualized by non-axisymmetric hot spots around the central zone.

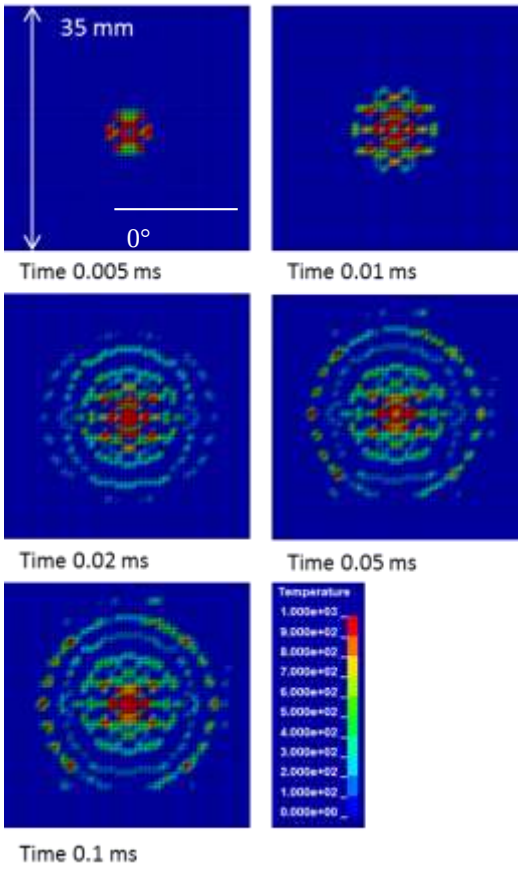

Figure 9 : Nodal temperature vs time in the 1st composite ply with the electromagnetic-thermal-mechanical model

It can be seen that the heating simulated by the model in the central zone elements does not reach the melting temperature of the copper on a surface as large as the area burnt in the test. However, hot spots appear along the path of the current propagation. The localization of these hot spots could explain local greater damage in the first composite ply and, in the case of paint, at the interface between the protective layer and the paint or in the paint itself.

These results are therefore encouraging, but show that even if the model is equivalent from a mechanical and electromagnetic point of view, it is necessary to represent

more precisely the geometry of the copper mesh if one wishes to represent the induced heating correctly.
Moreover, it should be noted that the presented model calculates only the Joule effects produced by the eddy current. On the one hand no explosion is taken into account. Liu et al. [10] demonstrated that local phenomena in the very beginning of the current delivery resemble an explosion. It will therefore be necessary to improve the model in this direction. On the other hand, the presence of the plasma column is not taken into account at all. It will be necessary to evaluate the influence of it, both on the electromagnetic coupling effects with the plate and on additional acoustic pressure and thermal loads.

We are now interested in the pressure generated on the first composite ply by heating the copper mesh layer. As a basis for comparison, we use the references [6-9,17].
Lepetit et al. [8] have shown that it is possible to reconstruct, by numerical simulation, the displacement and velocity profiles on the rear face of the composite plate recorded during a lightning shock using a purely mechanical model of equivalent pressure. The composite plate is modeled by a thin plate having an equivalent homogeneous elastic behavior determined in the framework of the classical laminate theory. We report on Figure 10 the spatio-temporal distribution of the pressure used in this reference for a plate protected with ECF195 then unpainted or painted with 200 µm of paint. For the unpainted plate with respect to a painted plate, the pressure is lower (1.7 MPa versus 16 MPa) but is applied over a longer period (30 µs versus 20 µs).

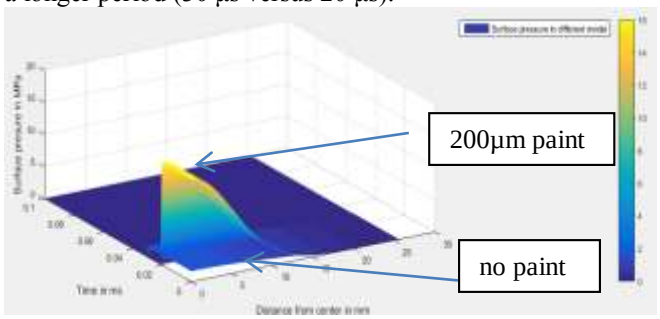

Figure 10 : Mechanical pressure distribution in space and time used in [8] to reproduce the rear face kinematics

The simulation work that we carried out previously [6,7] has demonstrated moreover that the total delaminated surface produced by a mechanical impact is of the same order of magnitude as the delaminated surface after a lightning shock even though the physics are very different. In their work, Karch et al. [9] and Soulas [17] obtain equivalent pressures with a more constricted profile at a peak value. The pressure proposed by Soulas [17] is represented on Figure 11.

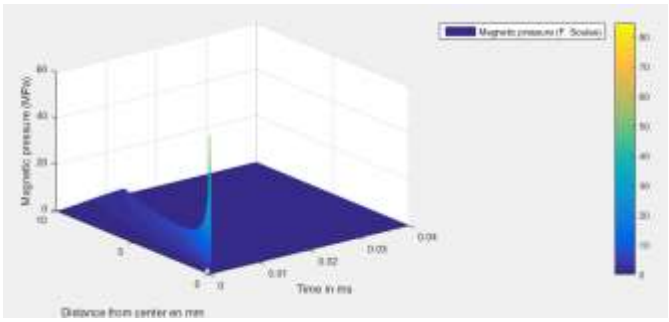

Figure 11 : Equivalent mechanical pressure distribution in space and time used in [17] to reproduce the impulse

We extracted from the results of our simulation the pressure applied over time by a line of copper elements on the upper surface of the elements of the first composite ply. A scheme similar to Figure 10 and Figure 11 Is proposed to compare the pressure obtained from our model. This illustration shows the pressure along the line as if the line was a radius and the distribution was axisymmetric. This is more or less the case before the maximum current value (before 20 µs), but is no longer so true after the peak because of the anisotropy of the current propagation which is at the origin of Joule effects. The comparison is illustrated on Figure 12, Figure 13 and Figure 14.

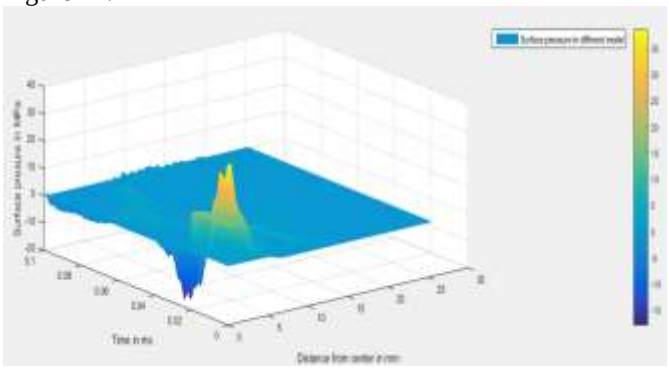

Figure 12 : Pressure distribution as a function of time and radius obtained by the coupled numerical model

Despite the oscillations due to a too coarse mesh, it is observed that the evolution of the pressure applied by the copper has three particular characteristics.

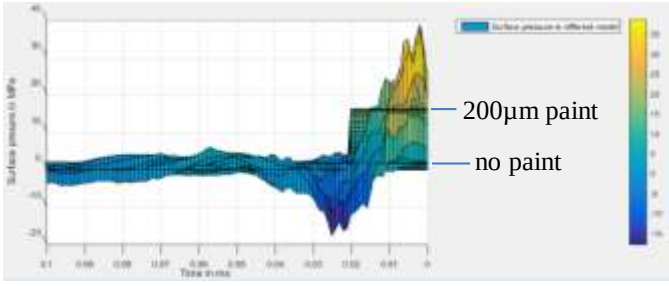

Figure 13 : Pressure distribution as a function of time obtained by the coupled numerical model

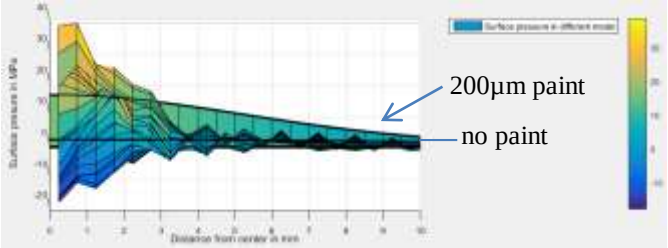

Figure 14 : Pressure distribution as a function of radius obtained by the coupled numerical model

First of all the maximum amplitude (almost 40MPa, Figure 13) is about 2.5 times the peak pressure value of the Lepetit model (Figure 10) for the painted plate and almost 24 times the value for the unpainted plate. The peak is however smaller than that of the pressure of Soulas (Figure 11) by a factor of 2/3. A generally increasing trend in the pressure amplitude for the first 5 to 10 microseconds can be observed over time, followed by a strong decrease indicating a vacuum when the current is no longer applied. On average, the duration of application is closer to the unpainted case of Lepetit. Depending on the radius (Figure 14), the pressure of the coupled model has a significant value up to a radius of the order of 3 to 4 mm rather close to the Soulas model, while it is maintained on a much larger radius (20 to 30mm) in the model of Lepetit. On average, the radius of application in our model is closer to the unpainted case of Lepetit, and the pressure of Soulas. The pressure distribution obtained by computation is therefore more complex than the analytical curves proposed so far, but presents similarities in both amplitude and spatial distribution.
Finally, velocities obtained in the panel over the first 20 microseconds (up to the maximum current) are compared on Figure 15 and Figure 16 to the actual lightning tests measures presented in the references [8,13]. Since the plate has small lateral dimensions compared to the test plate, only the maximum value given up to 20 µs or 25 µs can be compared. The velocity distribution at 10 µs shows that the surface load generates an anisotropic velocity in the thickness of the composite plate. This result is logical because the composite plies have an anisotropic mechanical behaviour. The velocities at the rear face follow a bell-shaped profile close to that observed in the tests. The distribution in the thickness will be used to simulate delamination later.

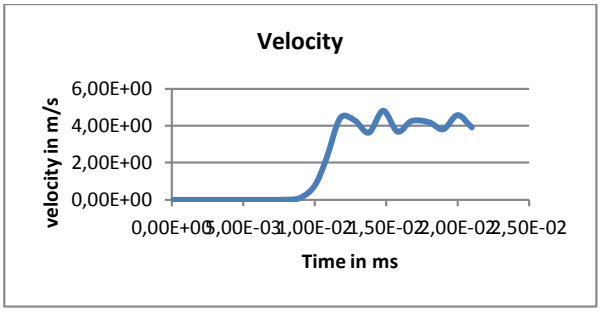

Figure 15 : Velocity at the centre of the rear face obtained by the coupled numerical model

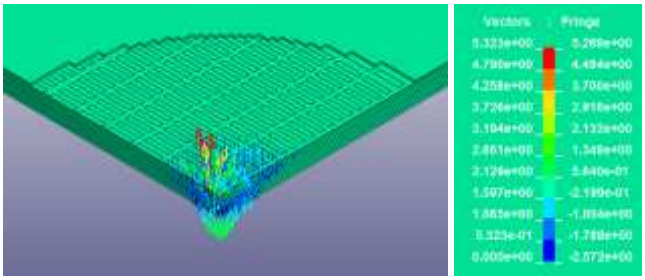

Figure 16 : Vertical velocity in the composite plate at 10µs by computed by the coupled numerical model

The maximum velocity at the center of the rear face of the composite plate (4.5 m / s) is about half the velocity measured during unpainted lightning test (10 m / s). This difference is attributed to the fact that we have not taken into account here the plasma column effects but only the Joule effects. The other half of the max displacements could be due to plasma coupling effects, including acoustic pressure and surface [4,18].

5 Conclusions

We presented in this paper a numerical simulation model using the strong coupling between the three solvers of the LS-DYNA® hydrodynamic code. This model has been developed to calculate the pressure and temperature produced by the Joule effect induced by eddy current injection. The pressure and temperature are applied by continuity to the upper face of the first ply of a composite plate that is protected and painted.
In our case we have modelled a painting spare in the center which makes our simulation closer to a case of lightning on an unpainted structure. We have obtained that the current flowing in the plate is responsible for a local heating much lower than the melting temperature because the temperature is solely due to Joule effect and then stops as soon as the current is no longer injected. If the model is able to represent on average the pressure produced over time and on a surface having a variable radius, the current alone cannot generate levels sufficient to explain the disappearance of the protective layer. Both explosive effects should be represented as proposed by Haigh [4] and Liu [10], as well as additional loads that act longer and over a wider radius. This longer duration of load and this wider radius are attributed to the plasma column interaction. It appears that the rear face velocity of the composite plate is about half the total speed of a real test, which leads us to conclude that 50% of the acceleration is due to resistive effects induced by the eddy current in the protective layer. This result is consistent with the results of Lepetit & al. [18].
The future models will allow the model to take account of more complex material model behaviours and the geometry of the metallic screening, but also of more dynamic effects of the loading (explosion).

Acknowledgements

All the technical staffs of AIRBUS, DGA-TA and ICA are thanked for their help and work in all experimental campaigns

presented in the present paper. Special Thanks to P. L'Eplattenier and I. Caldichoury of LSTC Corporation for their precious help in the use of the LS-DYNA® EM solver.

References

[1] A. B. Author, C. D. Author. "Title of the article", *The Journal*, **volume**, pp. 110-120, (2000).

1 G. Abdelal and A. Murphy, "Nonlinear numerical modelling of lightning strike effect on composite panels with temperature dependent material properties", *Composite Structures*, **109**, pp. 268–278, (2014).

2 T. Ogasawara, Y. Hirano, Yoshimura, "A coupled thermal–electrical analysis for carbon fibre/epoxy composites exposed to simulated lightning current". *Composites Part A* **41**, pp. 973–81, (2010).

3 Y. Hirano, S. Katsumata, Y. Iwahori and A. Todoroki, "Artificial lightning testing on graphite/epoxy composite laminate", *Composites Part A* **41**, pp. 1461–1470, (2010).

4 S. J. Haigh. "Impulse Effects during Simulated Lightning Attachments to Lightweight Composite Panels", Int. Conf. on Lightning and Static Electricity ICOLSE Paris (2007).

5 P. Feraboli and H. Kawakami. "Damage of Carbon/Epoxy composite plates subjected to mechanical impact and simulated lightning", *Journal of aircraft*, **47**, pp. 999-1012, (2010).

6 F. Soulas, C. Espinosa, F. Lachaud, Y. Duval, S. Guinard, B. Lepetit, I. Revel. "How to define a mechanical impact equivalent to a lightning strike", Int. Conf. on Lightning Static Electricity ICOLSE Toulouse (2015).

7 F. Soulas, C. Espinosa, F. Lachaud, Y. Duval, S. Guinard, B. Lepetit, I. Revel. "Approximation of a lightning test by a mechanical impact one: from equivalence criterion based on deflection to mechanical modelling of core damage and delamination", Int. Conf. on Lightning Static Electricity ICOLSE Toulouse (2015).

8 B. Lepetit, C. Escure, S. Guinard, I. Revel and G. Peres. "Thermo-mechanical effects induced by lightning on carbon fibre composite materials", Int. Conf. on Lightning Static Electricity ICOLSE Oxford (2011).

9 C. Karch, R. Honke, J. Steinwandel, KW. Dittrich. "Contributions of lightning current pulses to mechanical damage of CFRP structures", Int. Conf. on Lightning Static Electricity ICOLSE Toulouse (2015).

10 Z.Q. Liu, Z.F. Yue, J. Wang, Y.Y. Ji. "Combining analysis of coupled electrical-thermal and BLOW-OFF impulse effects on composite laminate induced by lightning strike", *Appl Compos Mater*, **22**, pp. 189-207, (2015). DOI 10.1007/s10443-014-9401-8

11 Q. Dong, Y. Guo, X. Sun, Y. Jia. "Coupled electrical-thermal-pyrolytic analysis of ac carbon fiber/epoxy composites subjected to lightning strike", *Polymer*, **56**, pp. 385-394, (2015). DOI 10.1016 / j.polymer.2014.11.029

12 R. Sousa Martins, L. Chemartin, C. Zaepffel, Ph. Lalande, A. Soufiani. "Electrical and hydrodynamic characterization of a high current pulsed arc", *J. Phys. D: Appl. Phys.*, **49**, pp. 185-204, (2016). DOI 10.1088 / 0022-3727/49/18/185204

13 F. Soulas, C. Espinosa, F. Lachaud, Y. Duval, S. Guinard, B. Lepetit, I. Revel. "Design of mechanical impact tests equivalent to lightning strikes", 16th European Conference on Composite Materials ECCM16 Seville (2014).

14 P. L'Eplattenier, G. Cook, C. Aschcraft. "Introduction of an Electromagnetism Module in LS-DYNA for Coupled Mechanical Thermal Electromagnetic Simulations", 3rd International Conference on High Speed Forming, 2008

15 LSTC, LS-DYNA Keyword User's Manual, ISBN 0-9778540-2-7

16 http://www.dexmet.com/1_pdf/Lightning%20Strike%20Brochure.pdf

17 F. Soulas, "Development of a lightning strike mechanical model for the prediction of damage of aeronautical composite panels", PhD Thesis Université de Toulouse, ICA/CNRS/ISAE-SUPAERO, 2016, 242p

18 B. Lepetit, F. Soulas, S. Guinard, I. Revel, G. Peres, Y. Duval, "Analysis of composite panel damages due to a lightning strike: mechanical effects", Int. Conf. on Lightning Static Electricity ICOLSE Seattle (2013).